Article

Impacts of Land-Use Changes on Soil Erosion in Water–Wind Crisscross Erosion Region of China

Jie Wang [1], **Weiwei Zhang** [2,*] **and Zengxiang Zhang** [3,4]

1   Department of Microbiology and Plant Biology, Center for Spatial Analysis, University of Oklahoma, Norman, OK 73019, USA
2   School of Environmental Science and Engineering, Suzhou University of Science and Technology, Suzhou 215011, China
3   Aerospace Information Research Institute, Chinese Academy of Sciences, Beijing 100101, China
4   University of Chinese Academy of Sciences, Beijing 100101, China
*   Correspondence: zhangweiwei@usts.edu.cn

check for updates

Abstract: Soil erosion affects food production, biodiversity, biogeochemical cycles, hydrology, and climate. Land-use changes accelerated by intensive human activities are a dominant anthropogenic factor inducing soil erosion globally. However, the impacts of land-use-type changes on soil erosion dynamics over a continuous period for constructing a sustainable ecological environment has not been systematically quantified. This study investigates the spatial–temporal dynamics of land-use change and soil erosion across a specific area in China with water–wind crisscross erosion during three periods: 1995–1999, 2000–2005, and 2005–2010. We analyzed the impacts of each land-use-type conversion on the intensity changes of soil erosion caused by water and wind, respectively. The major findings include: (1) land-use change in the water–wind crisscross erosion region of China was characterized as cultivated land expansion at the main cost of grassland during 1995–2010; (2) the strongest land-use change moved westward in space from the central Loess Plateau area in 1995–2005 to the western piedmont alluvial area in 2005–2010; (3) soil erosion area is continuously increasing, but the trend is declining from the late 1990s to the late 2000s; (4) the soil conservation capability of land-use types in water–wind crisscross erosion regions could be compiled from high to low as high coverage grasslands, medium coverage grasslands, paddy, drylands, low coverage grasslands, built-up lands, unused land of sandy lands, the Gobi Desert, and bare soil. These findings could provide some insights for executing reasonable land-use approaches to balance human demands and environment sustainability.

Keywords: land use; land cover; land degradation; land management; remote sensing

1. Introduction

Soil provides a variety of ecosystem services, such as sustaining food production, regulating climate and hydrological cycling, and supporting biodiversity [1]. Healthy soil is the basis of sustainability to ensure the security of food, water, and energy with an increasing population [2–4]. However, soil erosion is a major environmental problem threatening worldwide soil resources [5]. The soil erosion potential is increasing globally, particularly in Sub-Saharan Africa, South America, and Southeast Asia [2]. Soil erosion is a direct or indirect consequence of human activities, such as deforestation, overgrazing, unsuitable land-use practices, and climate change.

Soil erosion can be classified as water, wind, and freeze-thaw erosions, according to the formation mechanisms [6]. Water and wind erosions are driven by energy from rainfall and wind [5]. The potential of soil erosion is also determined by the topographic complexity, soil properties, land use, and

management practices [7,8]. Land-use change, a critical component of global change, regulates the effects of human activities on the conservation of soil and water resources. With increasing demands for food and settlements, natural vegetation (e.g., forest and natural grasslands) has been replaced by agricultural land and artificial surfaces, inducing expansion of soil erosion and reduction of soil resources [1,9]. Land use or management changes, such as increasing crop and grazing intensities, do not transfer the land cover types but potentially lead to soil property degradation with increasing erosion hazards [1].

In China, soil loss is one of the most critical environmental issues affecting agriculture productivity and the environment [10–13]. The arid and semi-arid regions of China are widely covered by the Gobi Desert, other desert areas, mobile sands, loess, and steppes, which are erodible landforms by water and wind [14–16]. In the Loess Plateau region, the average erosion rate could reach 30,000 t/km2.a [10]. This area is covered by fragile ecological systems (e.g., grasses and shrubs), which are very sensitive to human activities [15]. Anthropogenic land-use change is a dominant factor of accelerated soil erosion in these regions in the last several decades [15,17,18]. However, in 1999, the Grain-for-Green program was implemented to reconstruct the ecological environment to mitigate soil erosion at a national scale by increasing vegetation coverage [19–21]. In this project, the croplands with steep slopes were converted to grasslands and forested lands. The barren lands suitable for afforestation were planted by trees. There was about 4.5% coverage increase in grasslands and forested lands when this project is completed in 2010 [19]. Meanwhile, rapid urbanization and economic growth are driving the land-use changes across urban and rural areas in China [22,23]. Some studies have reported the improvement of soil and water conservation with vegetation restoration since 2000 [10,19,21]. Nevertheless, it is still unclear that the potential roles of various land-use and land-cover changes in regulating the dynamics of water and wind soil erosion. Systematic analysis on the responses of soil erosion to land-use and land-cover changes is crucial for balancing environment and human demands.

Water erosion affects a larger portion of earth's surface than wind erosion, but wind erosion severely exacerbates the environment in global arid and semi-arid regions [24]. To date, most of the studies on soil erosion are constrained to the regions dominated by water erosion [25–28]. We still lack studies to investigate the responses of wind erosion and water–wind crisscross erosion to land-use and land-cover change [15]. This study aimed to examine the overarching impacts of land-use changes on soil erosion controlled by the integrated effects of water and wind. The water–wind crisscross erosion region of China was selected as the study area. This area is consistent with the agriculture-grazing zone having a vulnerable ecosystem and intensive human activities and semi-arid and sub-humid climate. The specific objectives were to (a) examine the land-use dynamics and trends in the study area during 1995–2010; (b) estimate the soil erosion dynamics by water and wind during the study period; and (c) analyze the contributions of each land-use change to the intensity variations of water–wind crisscross erosion.

2. Materials and Methods

2.1. Study Area

The water–wind crisscross erosion region in China is located in the northern arid and semi-arid regions (39°N ~ 50°N,73°E ~ 125°E) (Figure 1). This area consists of 10 provinces with a total land area of about 252,000 km^2 and can be divided into the eastern plain sandy area, the central grassland sandy area, the central Loess Plateau area, and the western piedmont alluvial area. The topography is complex, mainly composed of mountains, hills, plateaus, and plains. It is in a transitional climate zone between the East Asian monsoon climate and the inland arid climate. From the northwest to the southeast, the average annual precipitation ranges from ~150 mm to ~450 mm, and the annual average wind speed is about 3–4 m/s, with gale mainly occurring in spring and fall [29–31]. This region belongs to the farming–pastoral zone from the view of land-use types [31,32]. Various climate, topography, and

land uses determine the water–wind crisscross erosion in this region [33,34]. Wind erosion dominates in spring and fall, and water erosion dominates in summer and winter [31,34].
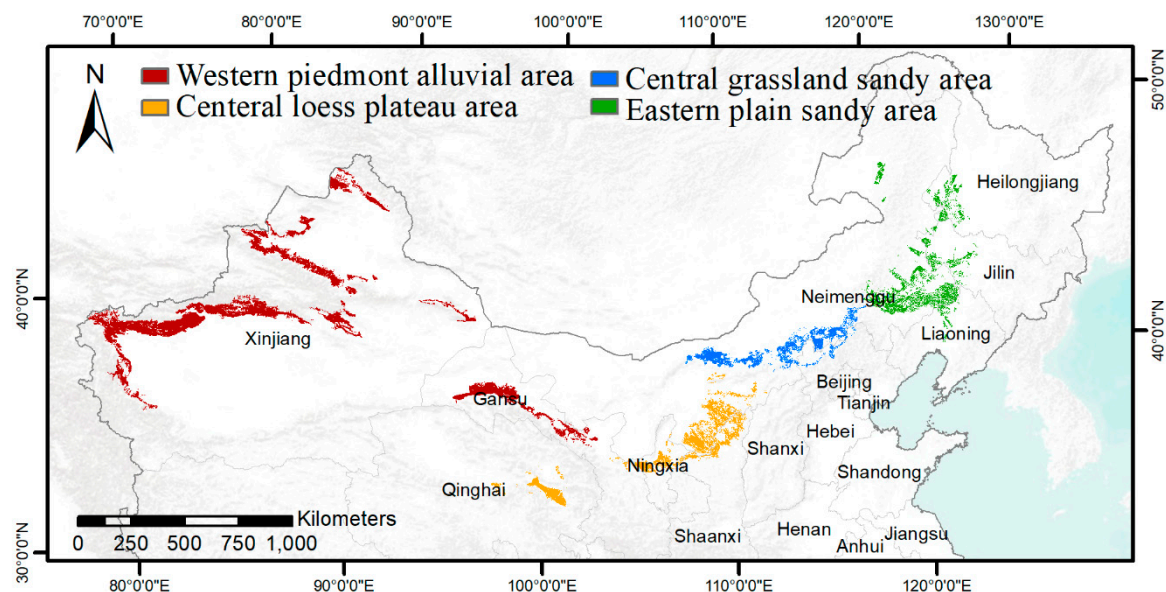

Figure 1. The water–wind crisscross erosion area in China. It consists of four regions from west to east: the western piedmont alluvial area, the central Loess Plateau area, the central grassland sandy area, and the eastern plain sandy area.

2.2. Data

2.2.1. Soil Erosion Dataset

The soil erosion status map in 1995 was used as a baseline in this study (Figure 2, Table S1). This satellite-based soil erosion product was developed in the second National Soil Erosion Investigation of China (NSEI-C) using field surveys and visual interpretation jointly by the Ministry of Water Resources (MWR) of the People's Republic of China and the Chinese Academy of Sciences (CAS). The soil erosion intensity was classified into six levels: slight, light, moderate, intensive, very intensive, and severe. The intensity of water–wind erosion was named by the levels of water erosion intensity and then followed by the levels of wind erosion intensity. We extracted the soil erosion status in 1995 for the water–wind crisscross erosion regions.

2.2.2. Land-Use Datasets from 1995 to 2010

This study used the dynamic vector database of National Land Use/cover Database of China (NLUD-C) for three periods: 1995–2000, 2000–2005, and 2005–2010 (Table S1). NLUD-C was produced mainly by the visual interpretation method from multi-source remote sensing data having a spatial resolution of around 30-m [35]. A hierarchical classification system was used for NLUD-C with six first-level and twenty-five second-level land-use types. The six first-level land-use types are cultivated lands, woodlands, grasslands, water bodies, built-up lands, and unused lands. During the data generation, strict quality control was conducted by repeated visual interpretation and field verification [35]. The first-level types of NLUD-C were assessed having an accuracy of more than 95.41% using the field samples [35]. More information about this database has been reported by Zhang, Wang, Zhao, Liu, Yi, Zuo, Wen, Liu, Xu and Hu [35].
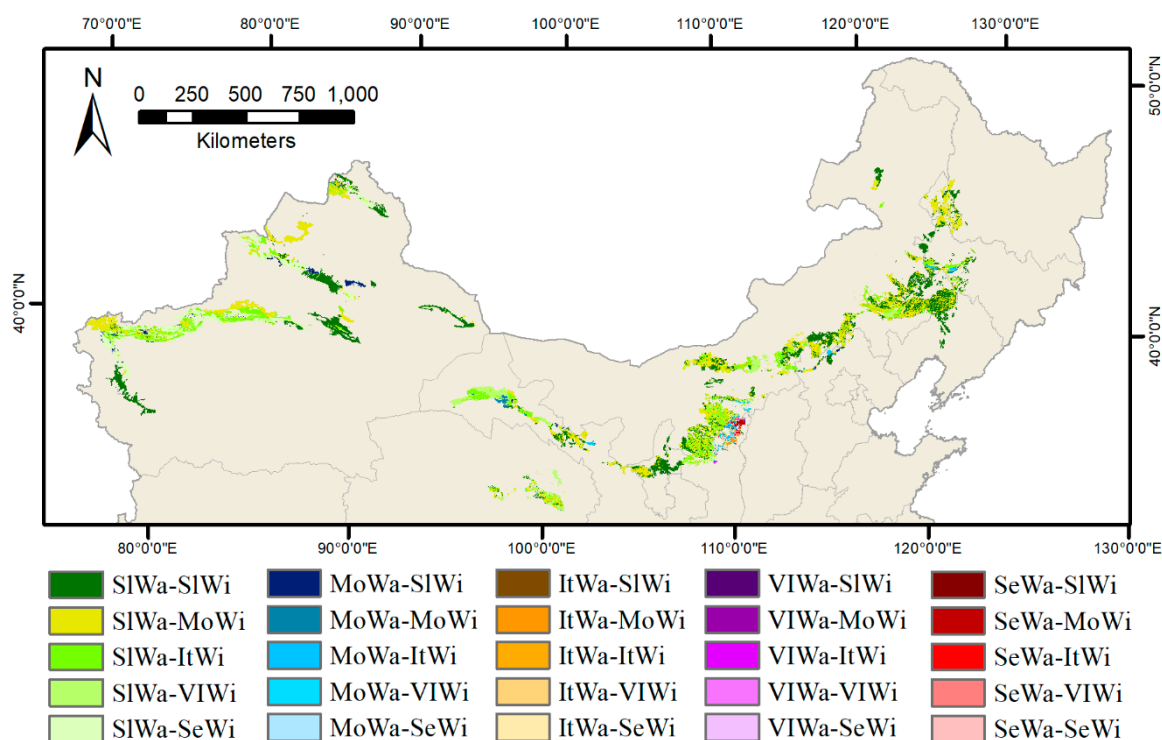
Figure 2. The soil erosion map in 1995 for the water–wind crisscross erosion area in China. This map shows the distribution of water erosion (Wa) and wind erosion (Wi) with five intensity levels of slight (Sl), Moderate (MO), Intensive (It), Very Intensive (VI), and Severe (Se). For example, "SlWa-MoWi" presents the region having water erosion intensity level of slight and wind erosion intensity level of moderate. The area of each soil erosion intensity level is summarized in Table S2.

2.2.3. Vegetation Index

Normalized difference vegetation index (NDVI) [36] presents the vegetation greenness and is commonly used to indicate the vegetation coverage. The 16-day Moderate Resolution Imaging Spectroradiometer (MODIS) vegetation indices product (MOD13Q1, V06) having a 250-m spatial resolution was used in this study (Table S1). This product has been widely used to analyze the vegetation dynamics over a variety of regions [37,38]. We calculated the annual maximum NDVI based on this dataset to delineate the vegetation coverage in the study area for three time points of 2000, 2005, and 2010.

2.2.4. Topography

Soil erosion varies with surface topography [39]. In this study, we used the 30-m ASTER Global Digital Elevation Map (ASTER GDEM V2, released in 2011) downloaded from NASA Earthdata (https://search.earthdata.nasa.gov/search) to describe the topography of the study area (Table S1).

2.2.5. Soil Survey Database

Soil property is a key factor that influences soil loss [8,27]. We obtained the 1-km national soil survey map of China from the Environment and Ecological Science Data Center for West China [18]. We examined the soil texture (% sand, silt, clay) to identify the soil physical properties within the water–wind crisscross erosion regions.

2.3. Methods

2.3.1. Analysis of Land-Use Dynamics

Land-use change was examined at two aspects: (1) area changes of each land-use type and (2) conversions among land-use types. We compiled statistics about the total area changes of each land-use type based on the NLUD-C dynamic datasets for the three study periods of 1995–2000, 2000–2005, and 2005–2010.

The transformational matrix is widely applied to analyze land-use conversions [40]. In this study, we used this approach to quantify the conversions among land-use types during three study periods, including conversions of land-use types and the associated area dynamics. We first constructed the land-use transformational matrix for each period based on the dynamic datasets of NLUD-C across the study area. We then compiled statistics about the total area change for each land-use type conversion. Based on the results of each period, we calculated the changes in land-use types and areas for the entire study period of 1995–2010.

2.3.2. Classification of Soil Erosion Intensity

The intensity of soil erosion was identified following the *Standards for classification and gradation of soil erosion* published by the MWR. In the decision rules, soil erosion intensity is mainly classified by the factors of land use, vegetation, slope, landforms, and soil properties (Table 1). These rules have been successfully implemented to generate the soil erosion maps of China since the 1980s [6]. According to these rules, we built up an expert decision system to grade the soil erosion intensity for the study area at the three time points of 2000, 2005, and 2010 (Figure 3).
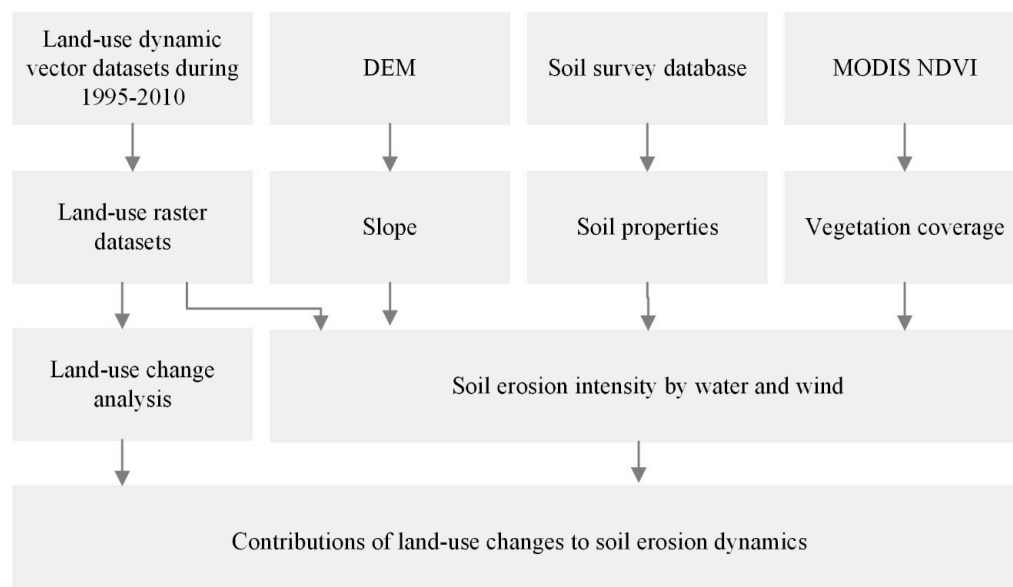

Figure 3. The workflow of this study mainly includes three analyses of land-use change, soil erosion intensity by water and wind, and the contributions of land-use changes to soil erosion dynamics. DEM = Digital Elevation Map; NDVI = normalized difference vegetation index.

In this decision system, the land-use dynamic datasets, vegetation coverage, topography, and soil data were used as inputs. These datasets have different data formats, including vector and raster (Table S1). Meanwhile, the original raster datasets have spatial resolutions from 30-m to 1-km (Table S1). To avoid the obstructions from these dataset inconsistencies for soil erosion assessment, we first converted the vector soil erosion map in 1995 and land-use maps during 1995–2010 into a raster format with a 100-m spatial resolution. Then, the 250-m MODIS NDVI, 30-m ASTER GDEM

V2, and 1-km soil survey map were resampled into 100-m by the nearest neighbor method to make all of these datasets having a consistent spatial resolution. Meanwhile, the resampled 100-m ASTER GDEM was used to produce a slope map in Arcmap for soil erosion analysis. After the preparation of these input datasets, we assessed the soil erosion intensity levels pixel by pixel. For each pixel, the soil erosion intensity levels by water and wind were determined separately, according to the rules in Table 1, including the land-use types, vegetation cover, slope, and sand content. Using this approach, 100-m soil water and wind erosion intensity maps were produced for 2000, 2005, and 2010. In these maps, six levels (including slight, light, moderate, intensive, very intensive, and severe) were used to delineate the soil erosion intensity by water and wind. Due to the study regions having water–wind crisscross erosion, we first classified the water erosion intensity and then graded the wind erosion intensity for each pixel. Thus, the soil erosion intensity in the results was named as water-erosion intensity followed by wind-erosion intensity.

In the rules, vegetation coverage was used to define the vegetation conditions on the ground. Vegetation coverage (f_g) can be derived from NDVI using the models provided by Gutman and Ignatov [41]). As most of the pixels have a mixed structure at the 250-m spatial resolution, we used the mosaic-pixel model to derive f_g from MODIS NDVI (Equation (1),(2)). In this model, the NDVI of a pixel was composed of NDVI from vegetation ($NDVI_g$) and non-vegetation ($NDVI_0$) parts allocated by the vegetation coverage within that pixel (f_g) (Equation (1)). Mathematically, Equation (1) can be transformed into Equation (2) to calculate f_g.

$$NDVI = f_g NDVI_g + (1 - f_g) NDVI_0, \tag{1}$$

$$f_g = \frac{NDVI - NDVI_0}{NDVI_g - NDVI_0}, \tag{2}$$

where *NDVI* denoted the actual NDVI of a given pixel which can be obtained from the MODIS product directly. f_g was the vegetation coverage in the given pixel. $NDVI_g$ denoted the NDVI of the given pixel under pure vegetation cover. $NDVI_0$ referred to the NDVI of the pixel without vegetation cover. Thus, $NDVI_g$ can be noted as the maximum NDVI of each land-use type, and $NDVI_0$ was defined as zero to present the surface without vegetation.

2.3.3. Effects of Land-Use Change on Soil Erosion Dynamics

Land-use changes are considered to be a key factor in soil erosion during a short period owing to changeable characteristics caused by human activities. Meanwhile, reasonable land uses may not affect or reduce soil erosion. A given change of soil erosion intensity could be associated with many cases of land-use transformations. Here, we use numbers of one to six to express the soil erosion intensity levels from slight to severe separately. The differences in the intensity levels between the later and the former period were used to show the changes in soil erosion intensity. Thus, we can compile statistics about the contributions of land-use transformations to the level changes of soil erosion intensity to study the relationships.

Table 1. The intensity of soil erosion was identified following the *Standards for classification and gradation of soil erosion* published by the Ministry of Water Resources (MWR). In the decision rules, soil erosion intensity is mainly classified by the factors of land use, vegetation, slope, and soil properties. VC presents vegetation cover, and SC denotes sand content.

Level	Water Erosion	Wind Erosion
Slight	Water bodies, built-up areas, paddy fields, swampland; woodland or grassland with VC greater than 75% or slope less than 5°; cultivated land with slope less than 5°	Water bodies, paddy fields, built-up areas, swampland; SC is less than 55% and VC is greater than 50%
Light	Woodland or grassland with VC of 60%–75% and slope of 5°–25°; VC of 45%-60% and slope of 5°–15°; VC of 30%–45% and slope of 5°–8°; cultivated land with slope of 5°–8°	SC is less than 55% and VC is of 20%–50%; SC is greater than 55% and VC is greater than 70%
Moderate	Woodland or grassland with VC of 60%–75% and slope larger than 25°; VC of 45%–60% and slope of 15°–35°; VC of 30%–45% and slope of 8°–15°; VC less than 30% and slope less than 15°; cultivated land with slope of 8°–15°	SC is less than 55% and VC is of 10%–20%; SC is greater than 55% and VC is of 50%–70%
Intensive	Woodland or grassland with VC of 45%–60% and slope larger than 35°; VC of 30% - 45% and slope of 25°–35°; VC less than 30% and slope of 15°–25°; cultivated land with slope of 15°–25°	SC is greater than 55% and VC is of 5%–10%; built-up area under construction; saline-alkali land
Very intensive	Woodland or grassland with VC of 30%–45% and slope larger than 35°; VC less than 30% and slope of 25°–35°; cultivated land with slope of 25°–35°	SC is greater than 55% and VC is of 5% - 10% and VC is of 1%–5%; bare land with SC less than 55%
Severe	Woodland or grassland with VC less than 30% and slope greater than 35°; cultivated land with slope greater than 35°; loess plateau in broken terrain with VC less than 10%, bare soil with slope greater than 8° or sand with slope greater than 25°	SC is greater than 55% and VC is less than 1%; Gobi Desert, and bare soil with SC greater than 55%

3. Results

3.1. Land-Use Changes during 1995 to 2010

From 1995 to 2010, about 13,893.16 km^2 of area has experienced land-use change including the first-level and second-level land-use types (Figure 4). From the first period of 1995–2000 to 2000–2005 and 2005–2010, the changing area dropped continuously, from about 6683.94 km^2 to 5202.28 km^2 and then 2006.94 km^2. During the 15 years, grasslands had the largest changes in the area, with a decrease of 3350.74 km^2 (Figure 5). It is followed by the increases of cultivated lands, woodlands, built-up lands, and water bodies. Unused land has the lowest net area change with a slight diminution of −56.6 km^2. A conspicuous feature for this period is the consecutive decline of grasslands and steady increments of cultivated lands, albeit the changing amounts are reducing for both types from the end of the 1990s to the end of the 2000s (Figure 5).

Transformational matrix analysis suggested the land-use transformations mainly happed on the grasslands, cultivated lands, and unused lands during the three study periods (Table 2). The dominant land-use transformations were grasslands to cultivated lands or unused lands, unused lands to grasslands or cultivated lands, and cultivated lands to grasslands. In the entire period, the area of grasslands to other land uses was the largest, while the declining trend for grassland slowed down (Figure 5). The transfer-in area from other land uses to cultivated lands was the largest in each period. The trend of cultivated land increment also slowed down. Grasslands provided the dominant land source for cultivated land expansion.

In the first two periods, the central Loess Plateau area experienced the highest land-use change, and the western piedmont alluvial area had the lowest land-use change (Figure 4a,b). However, in 2005–2010, the highest change happed in the western piedmont alluvial area, with a west moving trend in space (Figure 4c). These spatial dynamics demonstrate that the center of land-use changes in the study area was moving westward from the late 1990s to the late 2000s (Figure 4). In terms of the land-use transformations in each region, the transformations from grasslands to cultivated lands or unused lands were dominant in the eastern plain sandy area. The development of unused lands to grasslands dominated the land-use changes in the regions of the central Loess Plateau area and the central grassland sandy area. The cultivated land expansion was the main land-use change in the western piedmont alluvial area at the cost of grassland reduction. Unused lands also contributed to the increment of cultivated lands in this region.
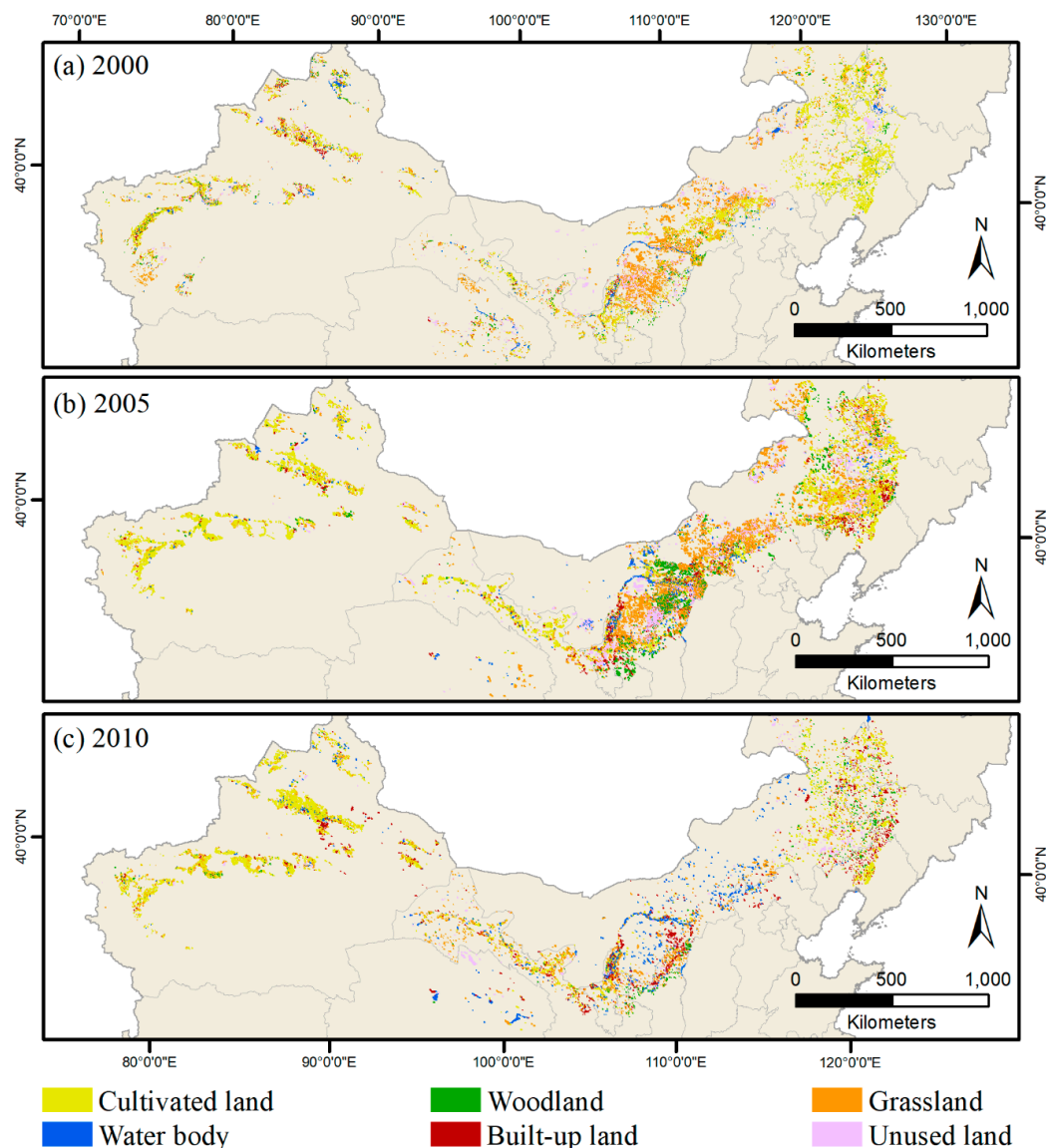

Figure 4. The distribution of land uses over the water–wind crisscross erosion area of China in (a) 2000, (b) 2005, and (c) 2010. Only the regions with land-use change during each period of 1995–2000, 2000–2005, and 2005–2010 were shown in these figures. The area of each land-use type is shown in Table S3. The differences in land-use change between 2000, 2005, and 2010 were shown in Figure S1.
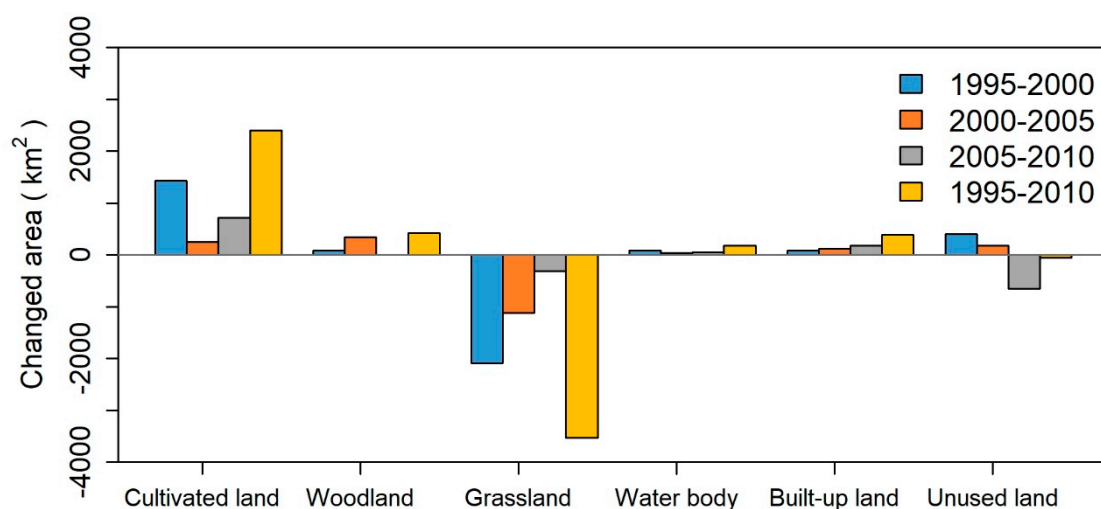
Figure 5. Changed area of each land-use type over the water–wind crisscross erosion region of China during four periods of 1995–2000, 2000–2005, 2005–2010, and 1995–2010.

Table 2. Land-use transformational matrix (area, unit: km^2) during three periods of 1995–2000 (1st), 2000–2005 (2nd), and 2005–2010 (3rd). Land-use types include cultivated lands (CL), woodlands (WL), grasslands (GL), water bodies (WB), built-up lands (BU), and unused lands (UL).

	CL			WL			GL			WB			BU			UL		
	1st	2nd	3rd	1st	2nd	3rd	1st	2nd	3rd	1st	2nd	3rd	1st	2nd	3rd	1st	2nd	3rd
CL	0	0	0	78.9	151.3	27.3	472.2	680.5	85.3	6.9	5.6	5.7	11.1	26.3	29.1	80.2	153.5	7.1
WL	87.0	50.5	15.02	0	0	0	12.8	57.2	8.1	1.5	1.5	0.2	0.4	2.9	2.4	5.9	16.2	3.7
GL	1942.2	863.3	511.5	77.0	274.4	6.4	0	0	0	60.4	19.4	13.4	49.5	64.7	93.1	715.7	934.5	165.0
WB	0	0	0	0	0	0	0	0	0	0	0	0	0	0	0	0	0	0
BU	0	0	0	0	0	0	0	0	0	0	0	0	0	0	0	0.2	0	0
UL	55.4	352.2	340.8	34.9	42.0	3.1	264.1	295.3	383.1	19.1	12.4	36.4	22.3	31.7	58.9	0	0	0

3.2. Dynamics of Soil Erosion During 1995 to 2010

The soil erosion maps in 2000, 2005, and 2010 were generated based on the land-use dynamics, vegetation coverage, slope, and soil properties by constructing a decision system following the Standards for classification and gradation of soil erosion published by the MWR (Figure 6, Table 1). During 1995–2010, the areas with intensity changes by water erosion and wind erosion were 7801.52 km^2 and 10,509.02 km^2, respectively.

From the first period to the third period, soil erosion in the study area can be summarized as exacerbation, slight exacerbation, and alleviation (Figure 7). Changes of water-erosion intensity concentrated on the levels of slight, light, moderate, and intensive. It can be generalized that light erosion was growing, and the moderate and intensive erosions were decreasing (Figure 7). In the first period, the growth of moderate and intensive water erosion was more significant than that of slight and light erosions. Water erosion was dramatically exacerbated in this period. In 2000–2005, although there was a decrease in moderate erosion, intensive erosion was not improved. Water erosion was still intensified in this period. In 2005–2010, erosion intensity shifted from intensive and moderate to slight and light, which suggested soil erosion was alleviated in this period. Changes of wind-erosion intensity distributed on all levels from slight to severe. In the three periods, wind erosion had consistent changing directions (e.g., exacerbation, slight exacerbation, and alleviation) with water erosion in spite of different changing levels. For example, in 1995–2000, intensive and very intensive wind erosions increased significantly, which were alleviated in 2000–2005. In 2005–2010, wind erosion in intensive, very intensive, and severe levels decreased, while that at light level increased dramatically.

Figure 8 shows the differences in soil erosion intensity for 1995–2000, 2000–2005, 2005–2010, and 1995–2010. The differences between water and wind soil erosion intensity mainly distributed on the unchanged, upper one, upper two, lower one and lower two levels. The differences in water–wind crisscross erosion intensity were mainly between the lower three to upper four levels. For the dynamics of water–wind erosion intensity in 1995–2010, the upgrade area (46%) was more than the degradation area (40%) by 6%, which suggests that soil erosion in this region was still intensified in the study period.
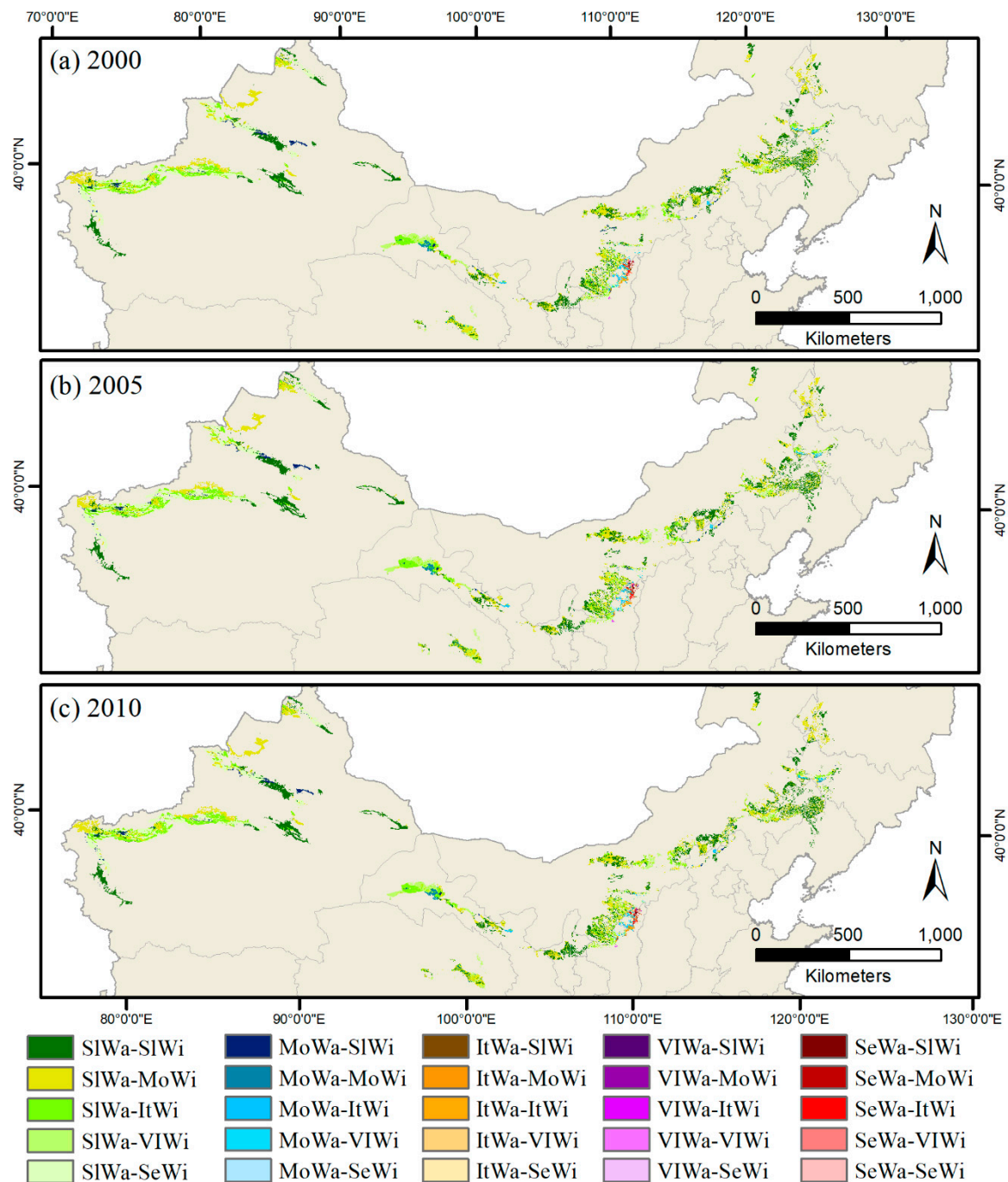

Figure 6. Distribution of water–wind erosion over the study area in three periods: (a) 1995–2000, (b) 2000–2005, and (c) 2005–2010. The legends are consistent with Figure 2. The area of each soil erosion intensity level is summarized in Table S2.
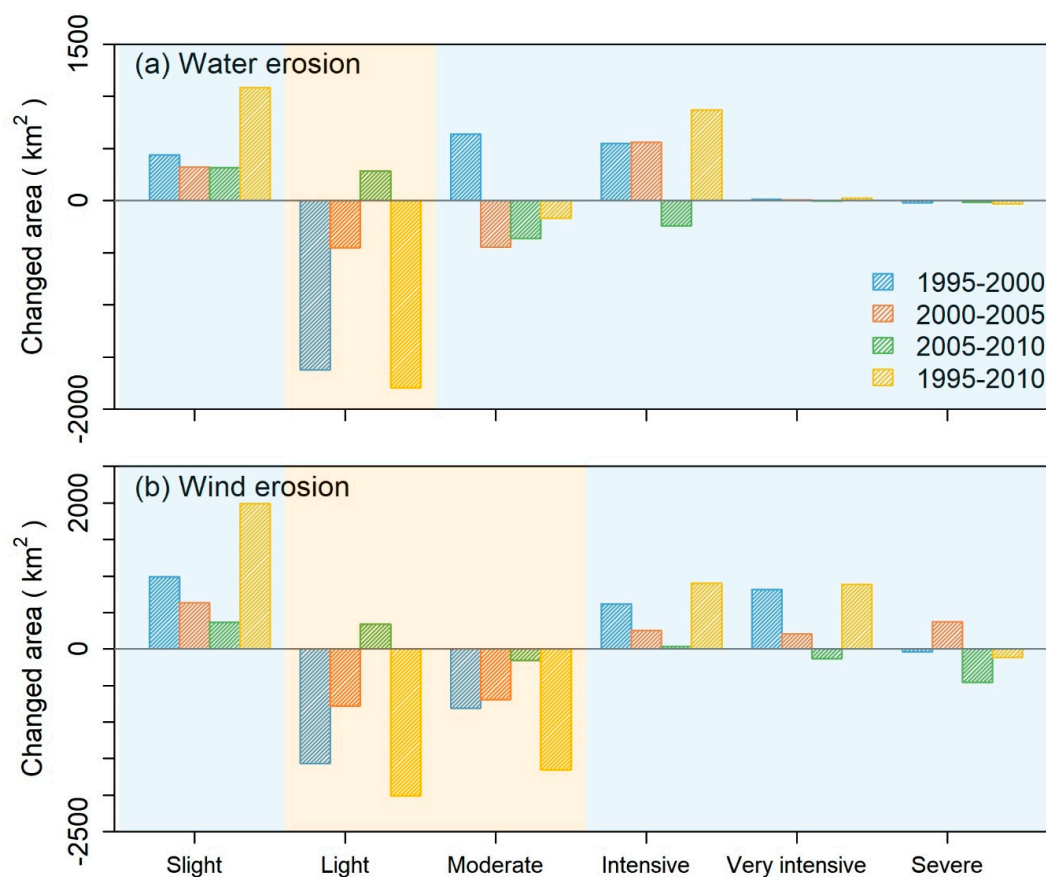
Figure 7. The net changed areas for each (**a**) water erosion and (**b**) wind erosion levels during for study periods of 1995–2000, 2000–2005, 2005–2010, and 1995–2010. The light blue and orange shadows present the decrease and increase trends of changed area for each intensity level during the three study periods.
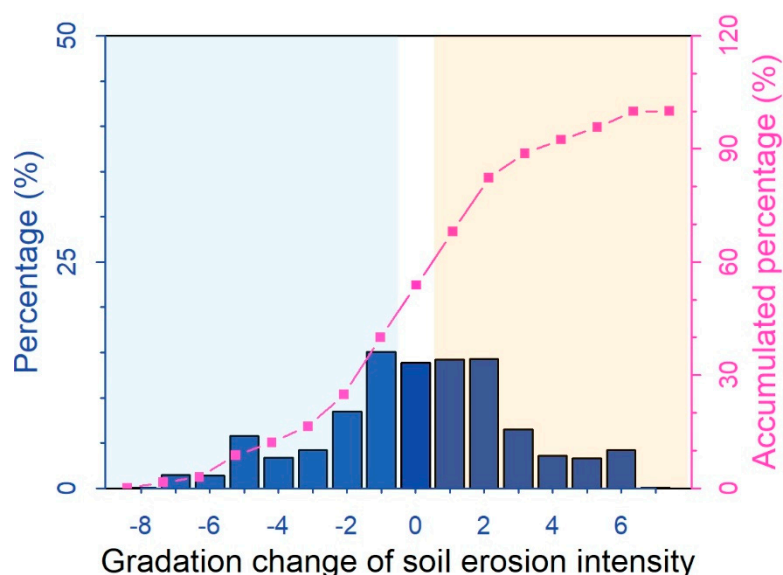

Figure 8. Percentage of each gradation change of water–wind combined erosion intensity across the water–wind crisscross erosion zone of China during 1995–2010. The accumulated percentage from gradation decrease to increase is shown in the purple line. The light blue and orange shadows highlight the intensity decrease and increase levels, respectively.

3.3. Contributions of Land-Use Changes to Soil Erosion Dynamics

Figure 9 shows the contributions of each land-use transformation to the intensity dynamics of water and wind soil erosion separately during three periods. The roles of land-use changes on the dynamics of water erosion intensity were affected by topography. For the regions with a slope less than 5°, no significant responses on erosion intensity were found to the transformations between grasslands and drylands. For the hillside lands, the conversion from medium or high coverage grasslands to drylands intensified the water erosion. In addition, the water erosion was also intensified with the conversions from medium or high coverage grasslands or drylands to low coverage grasslands, or unused lands of sandy lands, the Gobi Desert, bare lands (Figure 9a–c). Similarly, wind-erosion intensity was exacerbated by the transformations of high coverage grasslands to low coverage grasslands or drylands, drylands to low coverage grasslands, and grasslands to sandy lands. In comparison, it was more complicated for the responses of wind-erosion intensity to land-use changes as different effects can be found for a land-use conversion, like medium coverage grasslands and drylands (Figure 9d–f).

Figure 9g combined the intensity dynamics of water and wind soil erosions and summarized the land-use change types for erosion intensification and alleviation regions during 1995–2010. The results suggested that the land-use transformations may intensify the water–wind crisscross erosion including high coverage grasslands to low coverage grasslands, medium or high coverage grasslands to drylands, grasslands to unused lands of sandy lands, the Gobi Desert, and bare soil, drylands to low or medium coverage grasslands, and drylands to sandy lands or bare soil. The land-use transformation may improve the soil erosion in the study area including unused lands like sandy lands to grasslands, drylands or built-up lands, low coverage grasslands to high coverage grasslands or drylands, drylands to high coverage grasslands or paddy. Part of the land-use transformations may not affect the soil erosion including the coverage change of grasslands, and drylands to high coverage grasslands. In general, the soil conservation capability of land-use types in the study area could be compiled from high to low as high coverage grasslands, medium coverage grasslands, paddy, drylands, low coverage grasslands, built-up lands, unused lands of sandy lands, Gobi Desert, and bare soil. Here, the capability of built-up lands could vary with the vegetation coverage.
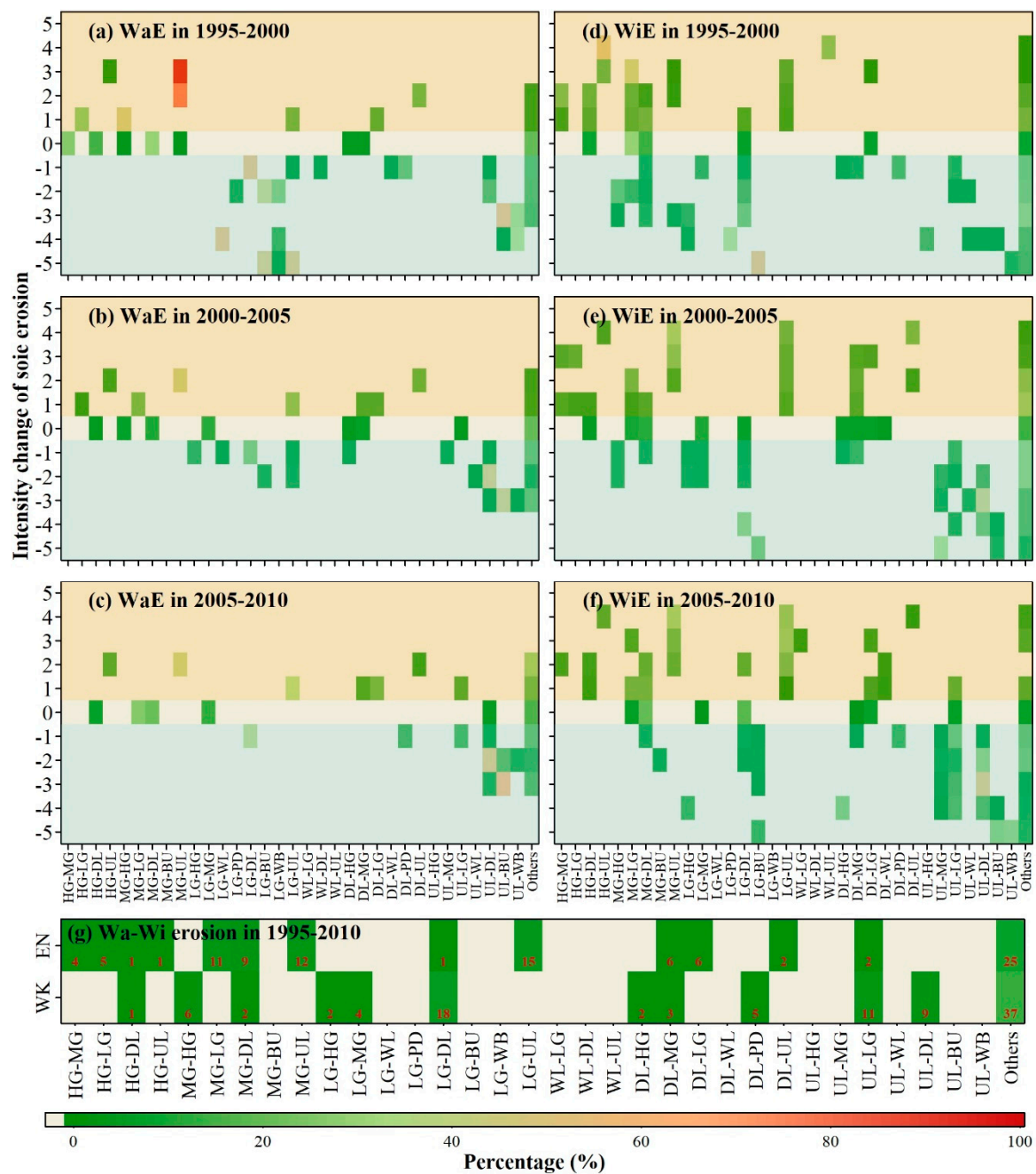
Figure 9. The contributions (noted by percentage) of each land-use transformation to every water (**a–c**) and wind (**d–f**) soil erosion intensity change during three periods. The light blue and orange shadows highlight the intensity decrease and increase levels, respectively. Figure 9g summarizes the contributions (the percentage was noted as red numbers) of each land-use transformation to the intensification and alleviation from water–wind combined soil erosion during 1995–2010. This figure shows the dominate land-use transformations, including high, moderate, and low coverage grasslands (HG, MG, LG), paddy (PD), drylands (DL), built-up lands (BU), unused lands of sandy lands, the Gobi Desert, bare soil (UL), woodlands (WL), and water body (WB).

4. Discussion

4.1. Soil Erosion in Water–Wind Crisscross Erosion Region During 1995–2010

This study suggested that soil erosion continuously happened on the water–wind crisscross erosion region during 1995–2000; however, the issue has been mitigated evidently from the late 1990s to the late

2000s (Figures 6 and 7). Previous studies also reported that severe soil erosion happened in the period of 1995—2000, and a declined soil erosion trend was found after 2000 in the regions having water–wind crisscross erosion, for example, in Inner Mongolia [16,42] and the Loess Plateau of China [10,21,25]. These results agree well with our findings in this study. This could be explained by the soil and water conservation practices in China. The conservation practices have been divided into five stages since the 1950s, including initial preparation (1950s–1963), highly erodible soil control (1964–1978), comprehensive management of small watersheds (1979–1989), natural restoration (1990–1999), and ecological restoration (since 1999) [25]. In the ecological restoration period, the 'Grain-for-Green' project was launched for controlling soil erosion. In this project, a number of croplands were converted to forest and grassland, and the vegetation coverage was greatly promoted [18,25].

This study could be improved in our following works using new datasets and improved analysis approaches. Currently, we only examined the soil erosion dynamics in the water–wind crisscross erosion region of China from 1995 to 2010. The status and dynamics of land use and soil erosion in the study area after 2010, which will be analyzed in our following works based on the updated NLUD-C in 2015, is still uncertain. In addition, this study was conducted at a 100-m spatial resolution based on MODIS data to calculate the vegetation cover. To better understand the impacts of human activities on soil resources, this analysis can be implemented at a field scale by using Landsat and Sentinel-2 images to assess the ground vegetation cover [43]. Finally, this study used a statistic method to survey the relationships between land-use changes and soil erosion intensity dynamics. Model-based approaches have been used to characterize the effects of land-use changes on soil erosion at a regional scale [28,44,45]. Thus, this analysis could be improved by integrating these two approaches to obtain robust conclusions.

4.2. Effects of Land Use Change on Soil Erosion

The resultant maps clearly show that the highest land-use change moved westward in space from the central Loess Plateau area (CLPA) in 1995–2005 to the western piedmont alluvial area (WPAA) in 2005–2010 (Figure 4). From 1995 to 2010, the proportion of land-use change in WPAA was increasing, while that of the other three regions was declining (Figure 10a). We found consistent trends for the water and wind soil erosion dynamics across these four regions in the study period (Figure 10b). The WPAA region with increasing land-use change and soil erosion was taken as an example. The main land-use change was the cultivated land expansion by occupying grasslands (Figure 4), which can explain some soil erosion due to higher soil conservation capability generally from grasslands than cultivated lands [2,42].

Cropland expansion is a dominant land-use-change factor inducing worldwide soil erosion [2]. It was estimated that soil erosion potential may have increased by 17% due to cropland expansion in the last several decades [28]. In Inner Mongolia, China, extensive grassland and wetland areas were converted to cropland during 2000–2010, which accelerated land desertification and soil erosion in this region [16,42,46]. With increasing population, forests in slight slopes and valley areas were removed to develop croplands, causing severe soil erosion in the Loess Plateau, China [25]. In this study, we also found grasslands had the largest decrease in the water–wind crisscross erosion region in China during 1995–2010. Meanwhile, croplands experienced the largest increase by occupying other land-use types in each five-year period from 1995–2010. This land-use characteristic explains the continuous intensification of soil erosion in the study area, albeit the erosion trend decreased from 1995–2010.

This study suggested that the soil conservation capability of land-use types from high to low can be generalized as high coverage grasslands, medium coverage grasslands, paddy, drylands, low coverage grasslands, built-up lands, unused lands of sandy lands, the Gobi Desert, bare soil across the water–wind crisscross erosion region of China. Previous studies proposed that a natural vegetation reconstruction is an effective approach for soil erosion control and soil resource conservation in ecologically vulnerable regions [25]. As the study area is located in the arid and semi-arid climate zone, the ecological environment is vulnerable. Trees do not have good growth in some regions. Therefore,

natural vegetation, especially grasses, rehabilitation is the best way to maintain the sustainability of soil resources in this area.
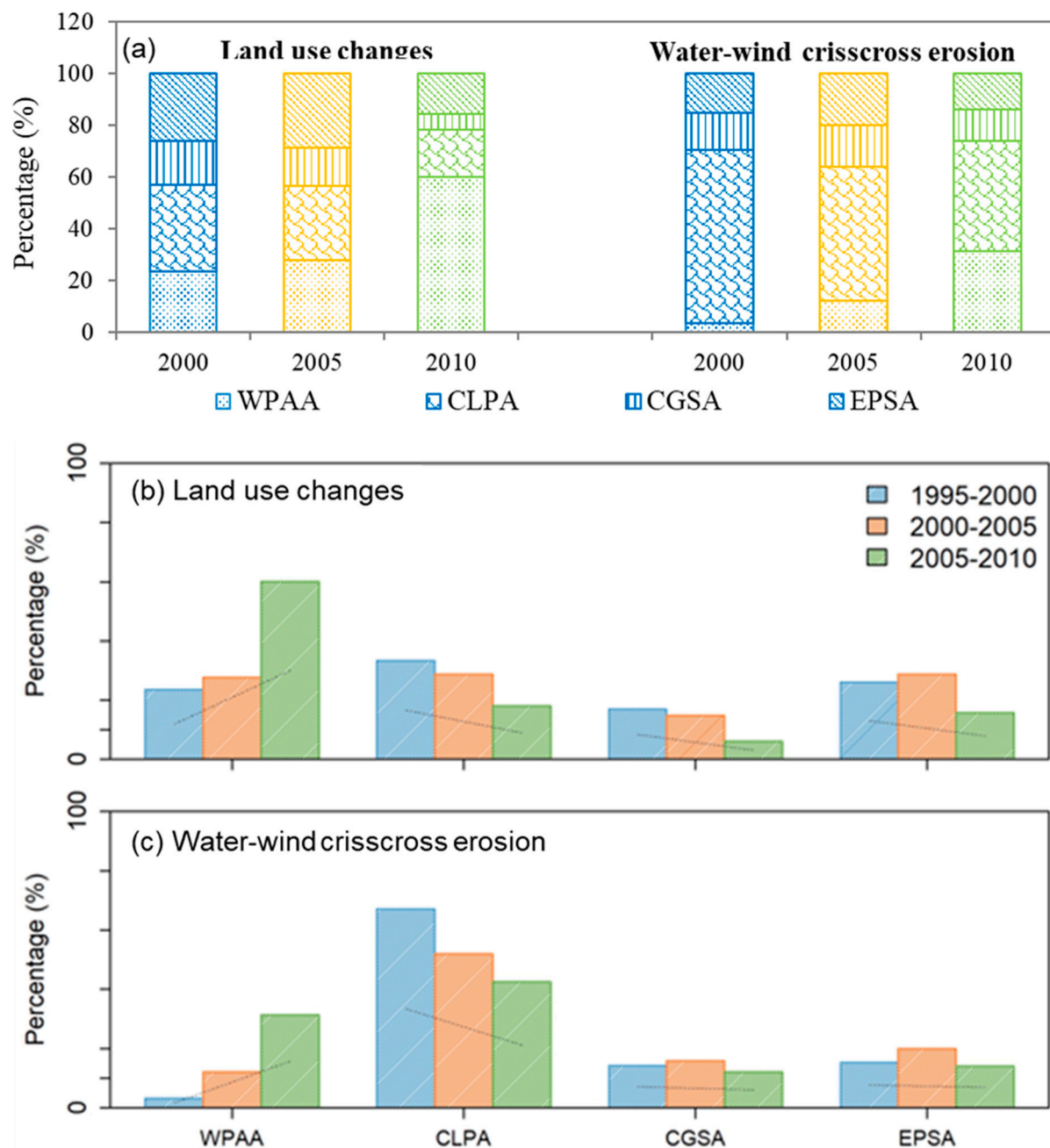

Figure 10. The (a) proportions and (b-c) trends of land-use changes and water–wind crisscross erosion across the four regions in the study area, including western piedmont alluvial area (WPAA), the central Loess Plateau area (CLPA), the central grassland sandy area (CGSA), and the eastern plain sandy area (EPSA).

5. Conclusions

Soil erosion is a global phenomenon, while the relationships between land-use changes and soil erosion dynamics have not been clearly quantified. We used remote sensing data to explore how land-use changes, soil erosion dynamics, and their relationships in water–wind crisscross erosion areas in China during 1995–2010. In general, soil erosion deteriorated continuously in the study area during 1995–2010, but the decreasing trend showed the ecological environment was improving. Grassland

decrease and cropland expansion were the most significant feature of the land-use change in this region. Meanwhile, the strongest land-use change and soil erosion were moving westward from the central Loess Plateau area to the western piedmont alluvial area. This spatial–temporal information provides references for performing ecological restoration projects across the study area in the future. The effect analysis of different land-use types suggested that restoration of medium and high grass cover is still necessary to conserve soil resources in the water–wind crisscross erosion area in China. These findings are a benefit for executing reasonable land-use management to balance human demands and environment sustainability.

Supplementary Materials: The following are available online at http://www.mdpi.com/2072-4292/11/14/1732/s1, Figure S1: Difference maps of land-use change between (a) the years of 2000 and 2005 and (b) the years of 2005 and 2010 (b). (c–d) show the zoom-in maps for the region highlighted by black rectangles in figure a, b, respectively. These figures show the regions experiencing land-use change only in 2000, 2005, 2010, and both in the years of 2000 and 2005, and both in the years of 2005 and 2010, Table S1: Datasets we used in this study, Table S2: Areas (km^2) of each soil erosion intensity level over the water-wind crisscross erosion area of China in 1995, 2000, 2005, and 2010. This table shows the soil erosion by water (Wa) and wind (Wi) with five intensity levels of slight (Sl), Moderate (MO), Intensive (It), Very Intensity (VI), and Severe (Se), respectively. For example, "SIWa-MoWi" presents the region having a water erosion intensity level of slight and wind erosion intensity level of moderate, Table S3: Areas (km^2) of each land-use type over the water-wind crisscross erosion area of China in 2000, 2005, and 2010. Only the regions experiencing land-use changes during the study periods of 1995–2000, 2000–2005, and 2005–2010 were examined.

Author Contributions: Conceptualization, W.Z., J.W. and Z.Z.; methodology, W.Z., J.W.; software, W.Z., J.W.; formal analysis, J.W. and W.Z.; investigation, J.W. and W.Z.; data curation, Z.Z.; writing—original draft preparation, J.W.; writing—review and editing, W.Z.; visualization, J.W.; project administration, W.Z.; funding acquisition, W.Z.

Conflicts of Interest: The authors declare no conflict of interest. The funders had no role in the design of the study; in the collection, analyses, or interpretation of data; in the writing of the manuscript, or in the decision to publish the results.

References

1. Smith, P.; House, J.I.; Bustamante, M.; Sobocka, J.; Harper, R.; Pan, G.X.; West, P.C.; Clark, J.M.; Adhya, T.; Rumpel, C.; et al. Global change pressures on soils from land use and management. *Glob. Chang. Biol.* **2016**, *22*, 1008–1028. [CrossRef] [PubMed]

2. Borrelli, P.; Robinson, D.A.; Fleischer, L.R.; Lugato, E.; Ballabio, C.; Alewell, C.; Meusburger, K.; Modugno, S.; Schütt, B.; Ferro, V.; et al. An assessment of the global impact of 21st century land use change on soil erosion. *Nat. Commun.* **2017**, *8*, 2013. [CrossRef]

3. Doran, J.W.; Zeiss, M.R. Soil health and sustainability: Managing the biotic component of soil quality. *Appl. Soil Ecol.* **2000**, *15*, 3–11. [CrossRef]

4. Gholoubi, A.; Emami, H.; Alizadeh, A. Soil quality change 50 years after forestland conversion to tea farming. *Soil Res.* **2018**, *56*, 509. [CrossRef]

5. Pimentel, D.; Harvey, C.; Resosudarmo, P.; Sinclair, K.; Kurz, D.; Mcnair, M.; Crist, S.; Shpritz, L.; Fitton, L.; Saffouri, R.; et al. Environmental and Economic Costs of Soil Erosion and Conservation Benefits. *Science* **1995**, *267*, 1117–1123. [CrossRef] [PubMed]

6. Wang, X.; Zhao, X.; Zhang, Z.; Yi, L.; Zuo, L.; Wen, Q.; Liu, F.; Xu, J.; Hu, S.; Liu, B. Assessment of soil erosion change and its relationships with land use/cover change in China from the end of the 1980s to 20010. *Catena* **2016**, *137*, 256–268. [CrossRef]

7. Millward, A.A.; Mersey, J.E. Adapting the RUSLE to model soil erosion potential in a mountainous tropical watershed. *Catena* **1999**, *38*, 109–129. [CrossRef]

8. Angima, S.; Stott, D.; O'Neill, M.; Ong, C.; Weesies, G.; Stott, D. Soil erosion prediction using RUSLE for central Kenyan highland conditions. *Agric. Ecosyst. Environ.* **2003**, *97*, 295–308. [CrossRef]

9.   Vanwalleghem, T.; Gomez, J.; Infante-Amate, J.; De Molina, M.G.; Vanderlinden, K.; Guzmán, G.; Laguna, A.; Giráldez, J. Impact of historical land use and soil management change on soil erosion and agricultural sustainability during the Anthropocene. *Anthropocene* **2017**, *17*, 13–29. [CrossRef]

10. Chen, N.; Ma, T.; Zhang, X. Responses of soil erosion processes to land cover changes in the Loess Plateau of China: A case study on the Beiluo River basin. *Catena* **2016**, *136*, 118–127. [CrossRef]

11. Liu, J.G.; Diamond, J. China's environment in a globalizing world. *Nature* **2005**, *435*, 1179–1186. [CrossRef] [PubMed]

12. Huang, J.; Rozelle, S. Environmental Stress and Grain Yields in China. *Am. J. Agric. Econ.* **1995**, *77*, 853. [CrossRef]

13. Lu, Y.; Jenkins, A.; Ferrier, R.C.; Bailey, M.; Gordon, I.J.; Song, S.; Huang, J.; Jia, S.; Zhang, F.; Liu, X.; et al. Addressing China's grand challenge of achieving food security while ensuring environmental sustainability. *Sci. Adv.* **2015**, *1*, e1400039. [CrossRef] [PubMed]

14. Wang, H.; Jia, X.; Li, K.; Li, Y. Horizontal wind erosion flux and potential dust emission in arid and semiarid regions of China: A major source area for East Asia dust storms. *Catena* **2015**, *133*, 373–384. [CrossRef]

15. Dong, Z.B.; Wang, X.M.; Liu, L.Y. Wind erosion in arid and semiarid China: An overview. *J. Soil Water Conserv.* **2000**, *55*, 439–444.

16. Wang, L.Y.; Xiao, Y.; Rao, E.M.; Jiang, L.; Xiao, Y.; Ouyang, Z.Y. An Assessment of the Impact of Urbanization on Soil Erosion in Inner Mongolia. *Int. J. Environ. Res. Public Health* **2018**, *15*, 550. [CrossRef]

17. Fu, B.J.; Wang, Y.F.; Lu, Y.H.; He, C.S.; Chen, L.D.; Song, C.J. The effects of land-use combinations on soil erosion: A case study in the Loess Plateau of China. *Prog. Phys. Geogr. Earth Environ.* **2009**, *33*, 793–804. [CrossRef]

18. Li, X.; Nan, Z.; Wu, L.; Ran, Y.; Wang, J.; Pan, X.; Wang, L.; Li, H.; Zhu, Z. Environmental and Ecological Science Data Center for West China: Integration and sharing of environmental and ecological data. *Adv. Earth Sci.* **2008**, *23*, 628–637.

19. Deng, L.; Shangguan, Z.P.; Li, R. Effects of the grain-for-green program on soil erosion in China. *Int. J. Sediment Res.* **2012**, *27*, 120–127. [CrossRef]

20. Deng, L.; Liu, G.B.; Shangguan, Z.P. Land-use conversion and changing soil carbon stocks in China's 'Grain-for-Green' Program: A synthesis. *Glob. Chang. Biol.* **2014**, *20*, 3544–3556. [CrossRef]

21. Fu, B.; Liu, Y.; Lü, Y.; He, C.; Zeng, Y.; Wu, B. Assessing the soil erosion control service of ecosystems change in the Loess Plateau of China. *Ecol. Complex.* **2011**, *8*, 284–293. [CrossRef]

22. Wang, J.; Zhang, W.; Zhang, Z. Quantifying the Spatio-Temporal Dynamics of Rural Settlements and the Associated Impacts on Land Use in an Undeveloped Area of China. *Sustainability-(Basel)* **2018**, *10*, 1490. [CrossRef]

23. Liu, Y.; Fang, F.; Li, Y. Key issues of land use in China and implications for policy making. *Land Use Policy* **2014**, *40*, 6–12. [CrossRef]

24. Lal, R. Soil Erosion by Wind and Water: Problems and Prospects. In *Soil Erosion Research Methods*; Routledge: Abingdon, UK, 2017; pp. 1–10.

25. Zhao, G.; Mu, X.; Wen, Z.; Wang, F.; Gao, P. Soil Erosion, Conservation, And Eco-Environment Changes in the Loess plateau of China. *Land Degrad. Dev.* **2013**, *24*, 499–510. [CrossRef]

26. García-Ruiz, J.M. The effects of land uses on soil erosion in Spain: A review. *Catena* **2010**, *81*, 1–11. [CrossRef]

27. Renard, K.G.; Foster, G.R.; Weesies, G.; McCool, D.; Yoder, D. *Predicting Soil Erosion by Water: A guide to Conservation Planning with the Revised Universal Soil Loss Equation (RUSLE)*; United States Department of Agriculture: Washington, DC, USA, 1997; Volume 703.

28. Yang, D.; Kanae, S.; Oki, T.; Koike, T.; Musiake, K. Global potential soil erosion with reference to land use and climate changes. *Hydrol. Process.* **2003**, *17*, 2913–2928. [CrossRef]

29. Ministry of Water Resources of the People's Republic of China; Chinese Academy of Engineering. *Soil Erosion Control and Ecological Security in China (Agro-pastoral Transitional Zone in Northern China)*; Science Press: Beijing, China, 2010.

30. Li, Z.G. *Quantitative Monitoring of Regional Soil Erosion*; Northwest A&F University: Yangling, China, 2001.

31. Yue, S.P.; Yang, R.X.; Yan, Y.C.; Yang, Z.W.; Wang, D.D. Spatial and temporal variations of wind erosion climatic erosivity in the farming-pastoral zone of Northern China. *Theor. Appl. Clim.* **2019**, *135*, 1339–1348. [CrossRef]

32. Liu, Z.J.; Liu, Y.S.; Li, Y.R. Anthropogenic contributions dominate trends of vegetation cover change over the farming-pastoral ecotone of northern China. *Ecol Indic* **2018**, *95*, 370–378. [CrossRef]

33. Song, Y.; Yan, P.; Liu, L. A review of the research on complex erosion by wind and water. *J. Geogr. Sci.* **2006**, *16*, 231–241. [CrossRef]

34. Wang, Y.Q.; Shao, M.A. Spatial Variability of Soil Physical Properties in a Region of the Loess Plateau of Pr China Subject to Wind and Water Erosion. *Land Degrad. Dev.* **2013**, *24*, 296–304. [CrossRef]

35. Zhang, Z.; Wang, X.; Zhao, X.; Liu, B.; Yi, L.; Zuo, L.; Wen, Q.; Liu, F.; Xu, J.; Hu, S. A 2010 update of National Land Use/Cover Database of China at 1:100000 scale using medium spatial resolution satellite images. *Remote Sens. Environ.* **2014**, *149*, 142–154. [CrossRef]

36. Tucker, C.J. Red and photographic infrared linear combinations for monitoring vegetation. *Remote Sens. Environ.* **1979**, *8*, 127–150. [CrossRef]

37. Ahl, D.E.; Gower, S.T.; Burrows, S.N.; Shabanov, N.V.; Myneni, R.B.; Knyazikhin, Y. Monitoring spring canopy phenology of a deciduous broadleaf forest using MODIS. *Remote Sens. Environ.* **2006**, *104*, 88–95. [CrossRef]

38. Galvão, L.S.; Dos Santos, J.R.; Roberts, D.A.; Breunig, F.M.; Toomey, M.; De Moura, Y.M. On intra-annual EVI variability in the dry season of tropical forest: A case study with MODIS and hyperspectral data. *Remote Sens. Environ.* **2011**, *115*, 2350–2359. [CrossRef]

39. McCool, D.K.; Brown, L.C.; Foster, G.R.; Mutchler, C.K.; Meyer, L.D. Revised Slope Steepness Factor for the Universal Soil Loss Equation. *Trans. ASAE* **1987**, *30*, 1387–1396. [CrossRef]

40. Liu, J.; Liu, M.; Zhuang, D.; Zhang, Z.; Deng, X. Study on spatial pattern of land-use change in China during 1995–2000. *Sci. China Ser. D Earth Sci.* **2003**, *46*, 373–384.

41. Gutman, G.; Ignatov, A. The derivation of the green vegetation fraction from NOAA/AVHRR data for use in numerical weather prediction models. *Int. J. Remote Sens.* **1998**, *19*, 1533–1543. [CrossRef]

42. Jiang, L.; Xiao, Y.; Zheng, H.; Ouyang, Z. Spatio-temporal variation of wind erosion in Inner Mongolia of China between 2001 and 2010. *Chin. Geogr. Sci.* **2016**, *26*, 155–164. [CrossRef]

43. Wang, J.; Xiao, X.; Bajgain, R.; Starks, P.; Steiner, J.; Doughty, R.B.; Chang, Q. Estimating leaf area index and aboveground biomass of grazing pastures using Sentinel-1, Sentinel-2 and Landsat images. *Isprs. J. Photogramm.* **2019**, *154*, 189–201. [CrossRef]

44. Feng, X.M.; Wang, Y.F.; Chen, L.D.; Fu, B.J.; Bai, G.S. Modeling soil erosion and its response to land-use change in hilly catchments of the Chinese Loess Plateau. *Geomorphology* **2010**, *118*, 239–248. [CrossRef]

45. Gessesse, B.; Bewket, W.; Brauning, A. Model-Based Characterization and Monitoring of Runoff and Soil Erosion in Response to Land Use/land Cover Changes in the Modjo Watershed, Ethiopia. *Land Degrad. Dev.* **2015**, *26*, 711–724. [CrossRef]

46. Montgomery, D.R. Soil erosion and agricultural sustainability. *Proc. Natl. Acad. Sci. USA* **2007**, *104*, 13268–13272. [CrossRef] [PubMed]